

ANL-HEP-PR-99-108
October 21, 2018

THE TRIPLE-REGGE TRIANGLE ANOMALY *

Alan. R. White[†]

High Energy Physics Division
Argonne National Laboratory
9700 South Cass, IL 60439, USA.

Abstract

It is shown that the triangle anomaly is present, as an infra-red divergence, in the six-reggeon triple-regge interaction vertex obtained from a maximally non-planar Feynman diagram in the full triple-regge limit of three-to-three quark scattering. A multi-regge asymptotic dispersion relation formalism can be used to isolate all anomaly contributions and to discuss when and how there is a cancelation.

*Work supported by the U.S. Department of Energy, Division of High Energy Physics, Contracts W-31-109-ENG-38 and DEFG05-86-ER-40272

[†]arw@hep.anl.gov

1. INTRODUCTION

In a companion paper to this[1] we demonstrate that in massless QCD certain reggeized gluon interactions contain an infra-red divergence that can be understood as the infra-red appearance[2] of the U(1) quark anomaly. Such vertices appear in a wide variety of multi-regge reggeon diagrams[3] and so this is a potential new manifestation of the anomaly in a dynamical role. Indeed we believe the appearance of the anomaly in this context is crucial for obtaining a unitary pomeron, together with confinement and chiral symmetry breaking, in (multi-)regge limits.

It is well-established that regge limits within QCD are described by reggeon diagrams[4]. Such diagrams involve reggeized gluon (or quark) propagators, reggeon interaction vertices, and external couplings to the scattering states, all of which are gauge invariant. In general, many Feynman diagrams give contributions to a single reggeon vertex - the BFKL kernel is a well-known example[4]. In this paper we illustrate the results of [1] by presenting an abbreviated version of the central calculation. We study the full triple-regge limit[5] of three-to-three quark scattering and show that the anomaly is present in the (six-reggeon) triple-regge interaction vertex obtained from a “maximally non-planar” Feynman diagram. In [1] we use an asymptotic dispersion relation formalism[6, 7] to show that in lowest-order the anomaly occurs only in such diagrams and in those related to them by reggeon Ward identities. Within this formalism, the anomaly appears because unphysical multiple discontinuities containing the necessary chirality transition contribute to the dispersion relation. For direct Feynman diagram calculations, its appearance can be understood as due to an unphysical singular configuration approaching the asymptotic region in which every propagator in a quark loop is on-shell and one propagator carries the zero momentum necessary for a chirality transition.

Even though the anomaly is present in a reggeon interaction it does not necessarily produce an effect in the amplitudes in which it is contained. Both the structure of external couplings and additional symmetries of the full reggeon diagrams can produce a cancellation. In particular, we show in [1] that when the scattering states are elementary quarks or gluons the anomaly always cancels in the full scattering amplitude. Indeed, in the lowest-order diagrams the symmetries of the transverse momentum integrations directly produce the cancellation. In general we expect such cancellations to extend to any process where the chirality violation involved can not be linked to (reggeized) gluon configurations with the quantum numbers of the winding-number current.

The anomaly does not cancel when a “reggeon condensate” with the quantum numbers of the winding-number current is present. It was argued in [3] that, in a

color superconducting phase with the gauge symmetry broken from $SU(3)$ to $SU(2)$, such a condensate is consistently reproduced in all reggeon states by anomaly infrared divergences, while also producing confinement, chiral symmetry breaking and a regge pole pomeron. $SU(3)$ gauge invariance should be obtained by critical pomeron behavior[8] in which the condensate and superconductivity simultaneously disappear. In [3] we assumed the existence of the anomaly together with a number of properties that the results of [1] show to be essentially correct, although there are significant differences. Once we have determined the full structure of the anomaly, we hope to implement the program of [3] in detail in future papers. If a unitary (reggeon) S-Matrix is obtained, as we anticipate, it will be very close to perturbation theory, with the non-perturbative properties of confinement and chiral symmetry breaking a consequence of the anomaly only.

We study the three-to-three scattering process illustrated in Fig. 1(a) and define momentum transfers Q_1, Q_2 and Q_3 as in Fig. 1(b).

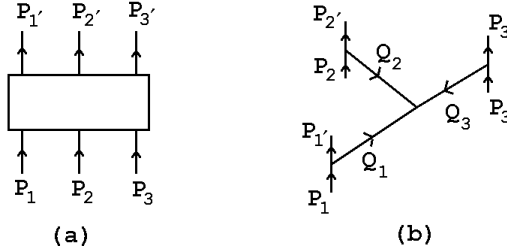


Fig. 1 Three-to-Three Scattering.

The full triple-regge limit[5] can be realized by taking each of P_1, P_2 and P_3 large along distinct light-cones, i.e.

$$\begin{aligned} P_1 \rightarrow P_1^+ &= (p_1, p_1, 0, 0), \quad p_1 \rightarrow \infty & Q_1 &\rightarrow (\hat{q}_1, \hat{q}_1, q_{12}, q_{13}) \\ P_2 \rightarrow P_2^+ &= (p_2, 0, p_2, 0), \quad p_2 \rightarrow \infty & Q_2 &\rightarrow (\hat{q}_2, q_{21}, \hat{q}_2, q_{23}) \\ P_3 \rightarrow P_3^+ &= (p_3, 0, 0, p_3), \quad p_3 \rightarrow \infty & Q_3 &\rightarrow (\hat{q}_3, q_{31}, q_{32}, \hat{q}_3) \end{aligned} \quad (1)$$

Momentum conservation requires that

$$\hat{q}_1 + \hat{q}_2 + \hat{q}_3 = 0, \quad \hat{q}_1 + q_{21} + q_{31} = 0, \quad \hat{q}_2 + q_{12} + q_{32} = 0, \quad \hat{q}_3 + q_{13} + q_{23} = 0 \quad (2)$$

and so there are a total of five independent q variables which, along with p_1, p_2 and p_3 , give the necessary eight variables.

Consider the maximally non-planar Feynman diagram shown in Fig. 2. In the limit (1), leading behavior is obtained when the quark loop remains at rest and the gluons are exchanged between the fast quarks and the loop. Some combination of

quark propagators will also be placed on (or close to) mass-shell by the limit. For the even signature amplitudes that we are interested in only on-shell (and not close to on-shell) propagators contribute and all gluons in the diagram are the lowest-order contribution of a reggeized gluon.

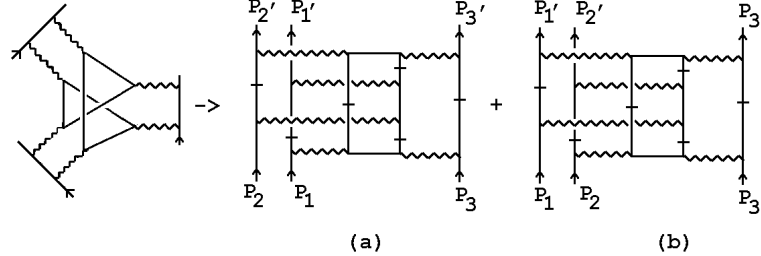


Fig. 2 Contributions from a Maximally Non-Planar Diagram

We discuss below how we determine whether a particular combination of on-shell propagators gives a relevant contribution. For the moment, we note only that Fig. 2(a) and (b) represent two possibilities. If we consider time to be in the vertical direction on the page then, a-priori, the hatched quark lines can naturally be close to mass-shell during the scattering. (Although, since the anomaly involves an unphysical chirality transition, we do not expect to find it in a succession of on-shell physical scattering process of this kind.) If we sum over quark directions, the loop lines hatched in Fig. 2(a) are the unhatched lines in Fig. 2(b). In either case, if we put all hatched lines on-shell and use the corresponding δ -functions to carry out longitudinal integrations in each of the external loops, we obtain a contribution to the lowest-order six-reggeon interaction as follows. We write $q_i = Q_i/2$, $i = 1, 2, 3$ and, for Fig. 2(a), label the gluon momenta as shown in Fig. 3(a). As is also shown in this figure, in the limit (1) the gluons couple to the quark loop via a “light-like” γ -matrix determined by the external momenta, i.e. $P_i^+ \rightarrow \gamma_{i-} = \gamma_0 - \gamma_i$, $i = 1, 2, 3$.

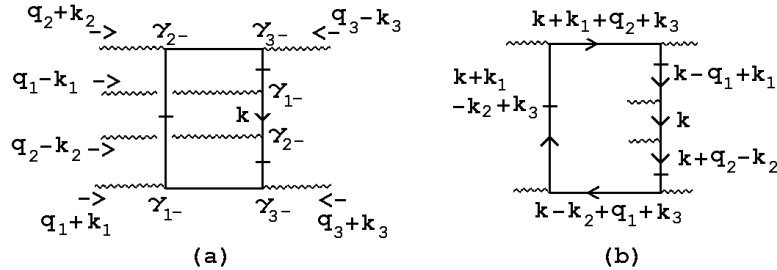


Fig. 3 (a) Gluon Momenta and γ -Matrix Couplings (b) Quark Loop Momenta

To carry out the longitudinal k_3 integrations we use conventional light-cone co-ordinates. For the k_1 and k_2 integrations we use special light-cone co-ordinates[1],

i.e. for a general four-momentum $p^\mu = (p_0, p_1, p_2, p_3)$ we write

$$p^\mu = p_{2-} \underline{n}_{1+} + p_{1-} \underline{n}_{2+} + \underline{p}_{12+}, \quad (3)$$

where $\underline{p}_{12+} = p_{12-} \underline{n}_{12+} + p_3 \underline{n}_3$ with $p_{12-} = p_1 + p_2 - p_0$, and

$$\underline{n}_{1+} = (1, 1, 0, 0), \quad \underline{n}_{2+} = (1, 0, 1, 0), \quad \underline{n}_{12+} = (1, 1, 1, 0), \quad \underline{n}_3 = (0, 0, 0, 1) \quad (4)$$

Analogous decompositions to (3) can also be introduced for γ -matrices.

With the hatched lines on-shell the quark loop reduces to a triangle diagram. With the light-cone co-ordinates we have chosen only the momentum routing of Fig. 3(b) produces the local (momentum independent) couplings at all three vertices[1] which are a prerequisite for the anomaly to be present. Apart from a normalization and color factor the asymptotic amplitude obtained is

$$\begin{aligned} & g^{12} \frac{p_1 p_2 p_3}{m^3} \times \\ & \int \frac{d^2 \underline{k}_{112+}}{(q_1 + \underline{k}_{112+})^2 (q_1 - \underline{k}_{112+})^2} \int \frac{d^2 \underline{k}_{212}}{(q_2 + \underline{k}_{212+})^2 (q_2 - \underline{k}_{212+})^2} \int \frac{d^2 \underline{k}_{33\perp}}{(q_3 + \underline{k}_{33\perp})^2 (q_3 - \underline{k}_{33\perp})^2} \\ & \int d^4 k \frac{\text{Tr}\{\hat{\gamma}_{12}(\not{k} + \not{k}_1 + \not{q}_2 + \not{k}_3 + m)\hat{\gamma}_{31}(\not{k} + m)\hat{\gamma}_{23}(\not{k} - \not{k}_2 + \not{q}_1 + \not{k}_3 + m)\}}{([k + k_1 + q_2 + k_3]^2 - m^2)(k^2 - m^2)([k - k_2 + q_1 + k_3]^2 - m^2)} + \dots \end{aligned} \quad (5)$$

where $k_{11-} = k_{22-} = k_{33-} = 0$, k_{12-}, k_{21-} and k_{33+} are determined by the mass-shell constraints that put propagators on-shell, and

$$\begin{aligned} \hat{\gamma}_{31} &= \gamma_{3-} \gamma_{2-} \gamma_{1-} = \gamma^{-,+,-} - i \gamma_5 \gamma^{-,-,-} \\ \hat{\gamma}_{23} &= \gamma_{2-} \gamma_{1-} \gamma_{3-} = \gamma^{+,-,-} - i \gamma_5 \gamma^{-,-,-} \\ \hat{\gamma}_{12} &= \gamma_{1-} \gamma_{3+} \gamma_{2-} = \gamma^{-,-,-} + i \gamma_5 \gamma^{-,-,+} \end{aligned} \quad (6)$$

with

$$\gamma^{\pm,\pm,\pm} = \gamma^\mu \cdot n_\mu^{\pm,\pm,\pm}, \quad n^{\pm,\pm,\pm\mu} = (1, \pm 1, \pm 1, \pm 1) \quad (7)$$

In that part of the amplitude not shown explicitly in (5) non-local (momentum dependent) couplings replace one, or more, of the $\hat{\gamma}$'s.

Writing $\alpha_i = \alpha((q_i + k_i)^2) + \alpha((q_i - k_i)^2) - 1$, $i = 1, 2, 3$, where $\alpha(t) = 1 + O(g^2)$ is the gluon regge trajectory, we have

$$\begin{aligned} p_1 p_2 p_3 &= (p_1 p_2)^{\frac{1}{2}} (p_2 p_3)^{\frac{1}{2}} (p_3 p_1)^{\frac{1}{2}} \sim s_{12}^{1/2} s_{23}^{1/2} s_{31}^{1/2} \\ &= (s_{13})^{(\alpha_1 + \alpha_3 - \alpha_2)/2} (s_{23})^{(\alpha_2 + \alpha_3 - \alpha_1)/2} (s_{12})^{(\alpha_1 + \alpha_2 - \alpha_3)/2} + O(g^2) \end{aligned} \quad (8)$$

where $s_{ij} = (p_i + p_j)^2$. This is the lowest-order triple-regge behavior for the amplitudes that interest us (and, in particular, potentially contain the anomaly). The transverse momentum integrals and gluon propagators in (5) can then be interpreted[1, 3] as the lowest-order contributions of two-reggeon states in each t_i ($= Q_i^2$)-channel. Removing these factors, the three γ_5 couplings in (6) give the $m = 0$ reggeon interaction

$$\begin{aligned} \Gamma_6(q_1, q_2, q_3, \tilde{k}_1, \tilde{k}_2, \underline{k}_{3\perp}, 0) = \\ \int d^4k \frac{Tr\{\gamma_5\gamma_{-,-,+}(\not{k} + \not{k}_1 + \not{q}_2 + \not{k}_3)\gamma_5\gamma_{-,-,-}\not{k}\gamma_5\gamma_{-,-,-}(\not{k} - \not{k}_2 + \not{q}_1 + \not{k}_3)\}}{(k + k_1 + q_2 + k_3)^2 k^2 (k - k_2 + q_1 + k_3)^2} + \dots \end{aligned} \quad (9)$$

corresponding to the triangle diagram of Fig. 4.

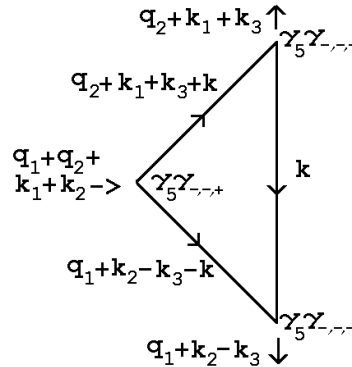


Fig. 4 The Triangle Diagram Corresponding to (9)

The maximal anomaly infra-red divergence[1, 2] of the axial-vector triangle diagram tensor $\Gamma^{\mu\nu\lambda}$ occurs in components with $\mu = \nu$ lightlike and λ an orthogonal spacelike index. In our case $\gamma_{-,-,-}$ appears at two vertices and this has a projection on the light-like vector $\underline{n}_{lc} = (1, \cos\theta_{lc}, \sin\theta_{lc}, 0)$. The $\gamma_{-,-,+}$ factor at the third vertex has a distinct projection on the orthogonal \underline{n}_3 direction. The anomaly produces a linear divergence[1, 2] when we take the limit

$$(k_1 + q_2 + k_3)^2 \sim (q_1 + q_2 + k_1 + k_2)^2 \sim (k_2 + q_1 - k_3)^2 \sim \mathbf{q}^2 \rightarrow 0 \quad (10)$$

of (9) while keeping a finite light-like momentum, parallel to \underline{n}_{lc} , flowing through the diagram. To show that this can be done with the mass-shell constraints satisfied, we define $\underline{n}_{lc\perp} = (0, -\sin\theta_{lc}, \cos\theta_{lc}, 0)$ orthogonal to \underline{n}_{lc} and take

$$\begin{aligned} q_1 + k_1 + q_2 + k_2 &= O(\mathbf{q}) \underline{n}_{lc\perp} \\ k_3 - k_2 - q_1 &= q_2 - k_2 + q_3 + k_3 = l \underline{n}_{lc} + O(\mathbf{q}) \underline{n}_{lc\perp} \\ q_2 + k_1 + k_3 &= k_1 - q_1 + k_3 - q_3 = l \underline{n}_{lc} + O(\mathbf{q}) \underline{n}_{lc\perp} \end{aligned} \quad (11)$$

We also take the loop momentum $k \sim O(\mathbf{q})$ and let $\mathbf{q} \rightarrow 0$ with

$$(q_1 - k_1) \rightarrow -2l (1, 1, 0, 0), \quad (q_2 - k_2) \rightarrow 2l (1, 0, 1, 0), \quad (12)$$

and

$$q_3 \rightarrow l (0, 1 - 1, 0), \quad k_3 \rightarrow l (0, 1 - 2\cos\theta_{lc}, 1 - 2\sin\theta_{lc}, 0) \quad (13)$$

In the limiting configuration the hatched lines of Fig. 2(a) are on-shell and in addition to $(q_1 + k_1)^2 = (q_2 + k_2)^2$ we also have $q_1^2 = q_2^2 = k_1^2 = k_2^2$. Only the lightlike momentum $k_{lc} = l \underline{n}_{lc}$ flows through the triangle graph of Fig. 4. The anomaly divergence appears, therefore, and the projection on \underline{n}_{lc} gives

$$\Gamma_6 \sim \frac{(1 - \cos\theta_{lc} - \sin\theta_{lc})^2 l^2}{\mathbf{q}} \quad (14)$$

It might appear that we have found the anomaly with the quark lines on-shell as a consequence of the physical scattering illustrated in Fig. 2(a). However, it is not difficult to show[1] that we have chosen what would be the unphysical pole (in this scattering) for the left-side propagator in the quark loop. In fact, the momentum configuration (12) and (13) actually describes the physical scattering illustrated in Fig. 5(a), if the time axis is vertical on the page.

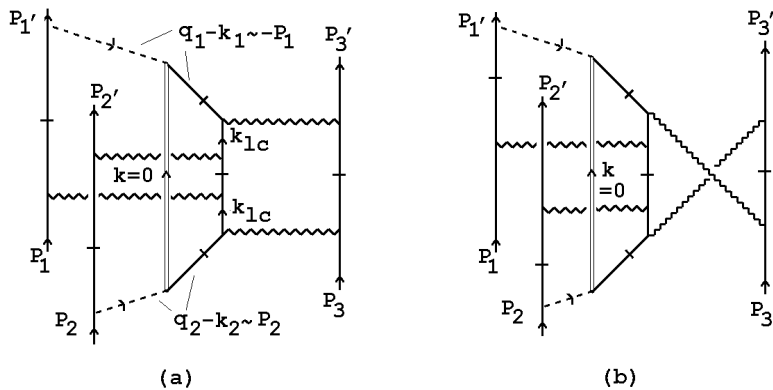


Fig. 5 Physical Scattering Processes Involving the Anomaly

This is the basic process associated with the anomaly in the reggeon vertex obtained from the lowest-order graphs. The dashed lines indicate light-like (“wee parton”) gluons, one incoming produced by an incoming quark and one outgoing that is absorbed by an outgoing quark. A zero-momentum quark (indicated by the open line) is emitted by the incoming wee-parton gluon, undergoes a chirality transition, and then is absorbed by the outgoing wee-parton gluon. The accompanying (on-shell) antiquark has its incoming light-like momentum pointed along \underline{n}_{lc} by scattering off a

spacelike gluon. It then forward scatters off two more spacelike gluons before another scattering points it's lightlike momentum in the outgoing direction.

Fig. 5(a) is quite distinct from the implicit time-ordering of Fig. 2(a) that we anticipated might place the hatched lines on-shell. In fact, in Fig. 5(a) the initial and final light-like anti-quarks are clearly not part of a physical intermediate state. Rather, the on-shell configurations enter the physical region only as the wee gluons become light-like. In the multi-regge dispersion relation formalism[1], that we briefly elaborate on below, all on-shell propagators are associated with some contributing discontinuity. If this discontinuity is not physical it must necessarily approach the physical region asymptotically, either from a cross-channel physical region as part of a physical multiple discontinuity (such discontinuities can not contain chirality transitions) or from an unphysical direction as part of an unphysical multiple discontinuity. For Fig. 5(a) the initial and final quark/antiquark pair can have the net chirality due to effective axial couplings only if the on-shell hatched lines represent unphysical discontinuities.

Before discussing the dispersion relation formalism we first consider diagrammatically how the anomaly might be canceled. Diagrams that contain the same quark loop divergence must be involved and an immediate possibility is the diagram and space-time scattering of Fig. 5(b). In an abelian theory Ward identities relating the diagrams of Fig. 5(a) and (b) at $(q_i \pm k_i)^2 = 0$, $i = 1, 2$ would produce a cancellation of the anomaly. With color factors, however, the two wee-parton gluons can form a color octet state in which the two diagrams do not cancel. The corresponding non-abelian (reggeon) Ward identities involve a triple gluon diagram that can not produce the chirality transition of the anomaly. Indeed, the failure of the reggeon Ward-identities can be regarded as the defining property that indicates the presence of the anomaly in the reggeon vertex.

There is, however, a relatively simple cancellation that occurs within the complete Feynman diagram (or more generally reggeon diagram) that contains the reggeon vertex. When the hatched lines of Fig. 2(b) are placed on-shell, the amplitude obtained differs only from that given by Fig. 2(a) in that the roles of P_1 and P_2 are interchanged, together with $k_1 \rightarrow -k_1$ and $k_2 \rightarrow -k_2$. In Fig. 5(a) the incoming and outgoing wee parton gluons are correspondingly interchanged. This interchange can be viewed as a (t -channel) parity transformation that produces a change of sign of the anomaly. After transverse momentum integration, the rest of the diagram is kinematically insensitive to this transformation and the anomaly is necessarily canceled.

In higher-orders the two gluons in each t_i channel are replaced by even signature two-reggeon states. If we keep the same quark loop interaction, the amplitude with even signature in each channel is obtained by summing over diagrams related by a twist in each t_i -channel. For external quark scattering, both the color factors and

all three of the k_i -integrations are then symmetric and the anomaly cancels. Sufficient antisymmetry to avoid cancelation would appear only if each of the even signature two-reggeon states carried negative color parity. However, anomalous color parity (i.e. \neq signature) reggeon states do not couple to elementary quarks (or gluons),

So far we have discussed only specific contributions from selected diagrams. In higher-orders, as both quarks and gluons reggeize, we expect the maximal non-planarity property to be necessary to produce, in each regge channel, the double spectral function property that is well-known to be required for regge cut couplings. In lowest-order we can not appeal to this expectation and, a-priori, all diagrams containing a quark loop and two gluons exchanged in each t_i channel could contribute. The total number of diagrams of this form is $O(100)$ and so studying them individually would clearly be difficult, if not impossible.

Fortunately, it is possible to systematically count all anomaly contributions by using the multi-regge asymptotic dispersion relation formalism developed in [6] and [7]. This is described in detail in [1] and here we give only a very brief discussion. The essential feature is that the asymptotic cut structure of amplitudes reduces to normal threshold branch-cuts satisfying the Steinmann relations, i.e. no double discontinuities in overlapping channels. Consequently the full amplitude can be written as

$$M(P_1, P_2, P_3, Q_1, Q_2, Q_3) = \sum_{\mathcal{C}} M^{\mathcal{C}}(P_1, P_2, P_3, Q_1, Q_2, Q_3) + M^0, \quad (15)$$

where M^0 contains all non-leading triple-regge behavior, double-regge behavior, etc. and the sum is over all triplets \mathcal{C} of three non-overlapping, asymptotically distinct, cuts allowed by the Steinmann relations.

When formulated in terms of angular variables the triple-regge limit is described as $z_i \rightarrow \infty$, $i = 1, 2, 3$, where $z_i = \cos\theta_i$ and θ_i is a t_i -channel scattering angle. If we consider only the z_i dependence, the asymptotic behavior of invariants is

$$\begin{aligned} s_{122'} &\sim s_{1'3'3} \sim -s_{1'22'} \sim -s_{13'3} \sim z_1 \\ s_{233'} &\sim s_{2'1'1} \sim -s_{2'33'} \sim -s_{21'1} \sim z_2 \\ s_{311'} &\sim s_{3'2'2} \sim -s_{3'11'} \sim -s_{32'2} \sim z_3 \\ s_{13} &\sim s_{1'3'} \sim -s_{13'} \sim -s_{1'3} \sim z_1 z_3 \\ s_{23} &\sim s_{2'3'} \sim -s_{23'} \sim -s_{2'3} \sim z_2 z_3 \\ s_{12} &\sim s_{1'2'} \sim -s_{12'} \sim -s_{1'2} \sim z_1 z_2 \end{aligned} \quad (16)$$

where, as above, $s_{ij} = (P_i + P_j)^2$, and in addition $s_{ij'} = (P_i - P_{j'})^2$, $s_{ijj'} = (P_i + P_j - P_{j'})^2$, etc. From (16) we find that all the asymptotic triple discontinuities are of one of the three forms, illustrated in Fig. 6 by tree diagrams in which an internal line represents a channel discontinuity. There are 24 of the first kind shown and 12 each of the second and third kinds. When the three invariants involved in an (a) or

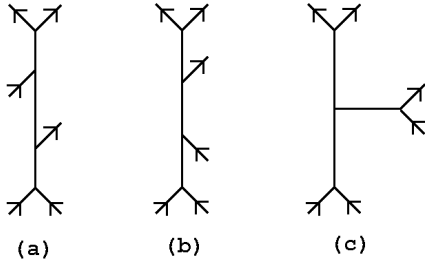


Fig. 6 Tree Diagrams for Triple Discontinuities.

(b) kind are each large and positive the z_i are always real and, as a result, such triple discontinuities lie in physical regions and include only on-shell configurations of the kind illustrated in Figs. 2(a) and (b). Crucially, however, asymptotic triple discontinuities of the (c) kind occur only in unphysical regions where the z_i are pure imaginary and some invariants (not giving a discontinuity) are also pure imaginary. Such unphysical discontinuities do not appear in simpler multi-regge asymptotic dispersion relations.

Unphysical discontinuities can not be discussed directly from an S-Matrix starting-point. However, the asymptotic dispersion relation can also be obtained[9] by starting with spacelike masses and utilising the primitive analyticity domains that follow from the field theory formalism of Generalised Retarded Functions[10]. The unphysical triple discontinuities appear just because they satisfy the Steinmann relations. These discontinuities are physical in two-four scattering processes and, in principle at least, S-Matrix “extended unitarity” equations can be derived from each of the three neighboring two-four regions for the three-three processes we discuss. It is then obvious that multiple discontinuities will be present combining processes from separate physical regions and in which chirality transitions can naturally occur.

To avoid introducing multi-regge theory in this paper we simply note that with the use of Sommerfeld-Watson representations and (the assumption of) regge behavior, the multiple discontinuities in the asymptotic dispersion relation can be converted to amplitudes that analytically continue away from the discontinuity region. To study the full triple-regge amplitude, therefore, it suffices to calculate all asymptotic triple discontinuities. Since there are only three distinct kinds, this is a much simpler proposition than the task of studying separately all Feynman diagrams.

The multi-regge representations for Fig. 6(b) and (c) are significantly different from that for Fig. 6(a). In particular, while the Fig. 6(a) discontinuities produce amplitudes with three possible signatures, each of the sets of Fig. 6(b) and (c) provide only four distinct signatured amplitudes. (We anticipate that the resulting “signature conservation” rule will lead to the even signature property of the pomeron when we finally extract the physical S-Matrix from reggeon diagrams.) Also the resulting

kinematic structure implies that the anomaly can appear only in the (b) or (c) types. The need for an unphysical chirality transition then selects the (c) type and it is possible to show that the anomaly arises only from discontinuities of this type and only from diagrams of the kind we have discussed. The above analysis can then be recast as the calculation of an unphysical multiple discontinuity followed by an extrapolation that gives the physical region anomaly amplitude of Fig. 5(a). The arguments for cancellation in the scattering of elementary quarks or gluons will apply.

References

- [1] A. R. White, hep-ph/9910458 (ANL-HEP-PR-99-102).
- [2] S. Coleman and B. Grossman, *Nucl. Phys.* **B203**, 205 (1982).
- [3] A. R. White, *Phys. Rev.* **D58**, 074008 (1998), see also Lectures in the Proceedings of the Theory Institute on Deep-Inelastic Diffraction, Argonne National Laboratory (1998).
- [4] E. A. Kuraev, L. N. Lipatov, V. S. Fadin, *Sov. Phys. JETP* **45**, 199 (1977); J. B. Bronzan and R. L. Sugar, *Phys. Rev.* **D17**, 585 (1978), his paper organizes into reggeon diagrams the results from H. Cheng and C. Y. Lo, *Phys. Rev.* **D13**, 1131 (1976), **D15**, 2959 (1977); V. S. Fadin and V. E. Sherman, *Sov. Phys. JETP* **45**, 861 (1978); V. S. Fadin and L. N. Lipatov, *Nucl. Phys.* **B477**, 767 (1996) and further references therein; J. Bartels, *Z. Phys.* **C60**, 471 (1993) and further references therein; A. R. White, *Int. J. Mod. Phys.* **A8**, 4755 (1993).
- [5] P. Goddard and A. R. White, *Nucl. Phys.* **B17**, 1, 45 (1970).
- [6] A. R. White, *Int. J. Mod. Phys.* **A11**, 1859 (1991); A. R. White in *Structural Analysis of Collision Amplitudes*, proceedings of the Les Houches Institute, eds. R. Balian and D. Iagolnitzer (North Holland, 1976); H. P. Stapp *ibid.*
- [7] H. P. Stapp and A. R. White, *Phys. Rev.* **D26**, 2145 (1982).
- [8] A. A. Migdal, A. M. Polyakov and K. A. Ter-Martirosyan, *Zh. Eksp. Teor. Fiz.* **67**, 84 (1974); H. D. I. Abarbanel and J. B. Bronzan, *Phys. Rev.* **D9**, 2397 (1974).
- [9] A. R. White, “The Past and Future of S-Matrix Theory”, hep-ph/0002303 (ANL-HEP-PR-00-011), to be published in “Scattering”, edited by E. R. Pike and P. Sabatier.
- [10] K. E. Cahill and H. P. Stapp *Ann. Phys.* **90**, 438 (1975).